Destabilization of a Faceted Smectic-A–Smectic-B Interface

Francisco Melo and Patrick Oswald
Laboratoire de Physique de L'Ecole Normale Supérieure de Lyon, 46 Allée d'Italie, Lyon CEDEX 07, France
(Received 17 October 1989)

We report observations of cellular growth at the smectic-B–smectic-A interface of the liquid crystal 4O.8. We link the existence of an angular discontinuity at the cell tips to the missing orientations in the equilibrium shape. The cell drift that we observe can be explained as resulting from the diffusion anisotropy in the smectic-A phase. Finally, we describe how facets destabilize.

PACS numbers: 61.30.Eb, 61.50.Cj

In previous work,[1] we reported the first observations of cellular and dendritic growth of the smectic-A–smectic-B (Sm-A–Sm-B) interface of 4O.8 (butyloxybenzilidene octylaniline) and showed that the impurity-diffusion version of the Mullins-Sekerka instability was responsible. We observed large differences between planar and homeotropic samples that we could not explain at the time. More recently, we investigated equilibrium surface properties. Our main results were as follows (see the photograph in the lower left corner of Fig. 1): (i) The interface is faceted parallel to the smectic layers. (ii) The facet matches tangentially with the contiguous curved regions. (iii) The face perpendicular to the smectic layers does not occur in the equilibrium shape, which has sharp edges. It corresponds to an unstable orientation.

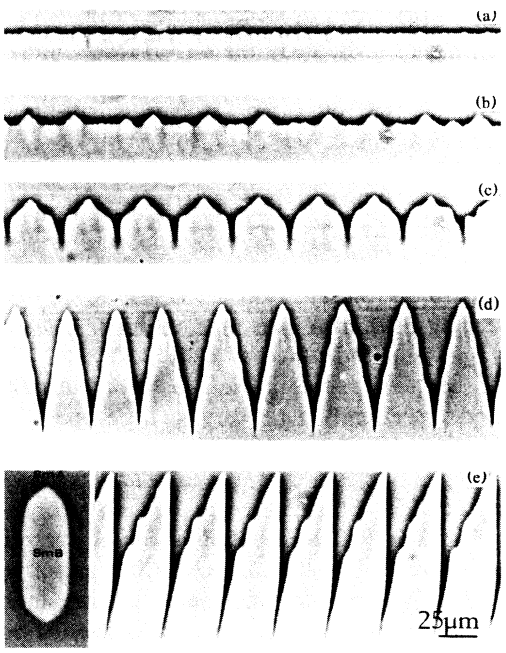

FIG. 1. Sm-A–Sm-B interface photographed via phase-contrast optics. The Sm-B is at the bottom and the Sm-A is at the top (the same in the other figures). For this sample, the temperature difference between liquidus and solidus lines is $\Delta T \approx 0.7$ K. The smectic layers are parallel to the temperature gradient, which is vertical ($G = 76$ K/cm). (a) Stationary interface: the hill-and-valley structure is clearly visible; (b), (c) $V = 0.38$ μm/s; (d),(e) $V = 0.45$ μm/s. Inset: A Sm-B monodomain in equilibrium with the Sm-A phase at constant temperature. The layers have the same orientation as those in (a)–(e).

In this Letter we study in detail how these surface properties influence the Mullins-Sekerka instability. We also analyze the role of impurity-diffusion anisotropy in the smectic-A phase as well as that of attachment kinetics of molecules on the interface. Below, we restrict ourselves to planar samples and describe the cellular bifurcation that occurs as the angle α between the layers and the normal to the macroscopic interface is varied. The cases corresponding to a forbidden orientation ($\alpha = 0°$) and to a facet ($\alpha = 90°$) will be separately described.

Our sample consists of two parallel glass plates separated by two 15-μm-thick spacers. Into the gap between the two plates we introduced the liquid crystal 4O.8, which has a Sm-A–Sm-B transition at 49.9 °C. To obtain planar alignment of the molecules on the glass (smectic layers normal to the glass), a 300-Å-thick layer of polyimide ZLI-2650 (Merck Corp.) was deposited on the inner surfaces. This layer was then rubbed in a single direction in order to orient the smectic layers perpendicular to the scratches.

Our directional solidification apparatus will be described in detail in a forthcoming publication. Briefly, one end of the sample is placed in a hot oven and the other end in a cold oven. The temperature gradient along the sample is measured with a thermocouple to about 5%. The sample is pushed by a fine screw that is driven by a stepping motor. The velocity ranges from 0.05 to 100 μm/s. Observations are made via phase-contrast microscopy.

The temperatures are chosen so that the Sm-A–Sm-B interface sits in the gap between the two ovens. The experiment consists of moving the sample at a constant velocity from the hot side to the cold. Thus we "freeze" the smectic-A, creating the smectic-B phase at a constant rate.

Let us first consider the case $\alpha = 0$ (layers parallel to the temperature gradient). Because the macroscopic interface is unstable ($\gamma + d^2\gamma/d\alpha^2 < 0$, where γ is the surface free energy), it breaks up into a hill-and-valley

© 1990 The American Physical Society

structure.[2] At rest and at small velocities, the amplitude of this modulation is of the order of a few μm [Fig. 1(a)]. At a critical velocity $V_c \approx 0.38$ μm/s, isolated triangular structures of finite amplitude develop [Fig. 1(b)]. These "triangles" grow and join to form a cellular front of large amplitude [Fig. 1(c)]. The cellular bifurcation is subcritical. The "brace"-shaped cells are pointed with an angular discontinuity at the tip, while the grooves between them are somewhat faceted. The cell amplitude increases rapidly with the velocity. Above $1.2V_c$, the cells become unstable and lateral undulations or sidebranches develop [Fig. 1(d)]. The branches appear alternately on one side of the cell and then on the other and so are out of phase. The sidebranch correlation extends across many cells (at least ten in our experiment). We also observed asymmetrical cells composed of a large, single facet and a rough, unstable part [Fig. 1(e)]. There is still an angular discontinuity at the tip and the sidebranches are strongly correlated, as for symmetrical cells. These cells drift slowly in time because of the symmetry breaking and the growth of the facet. This point is discussed below in more detail. We observe this solution always after a very long transient (several hours), and it seems to be more stable than the symmetric one. Similar translations of cellular patterns have also been observed in directional growth of the nematic-isotropic interface[3] and in a directional-fingering experiment.[4]

Many points should be emphasized.

(1) The existence of an angular discontinuity at the cell tip. Thus, orientations that are unstable at equilibrium do not appear during slow growth. This justifies the usual assumption of local thermodynamic equilibrium.

(2) The tendency to faceting responsible for asymmetrical cells.

(3) The existence of sidebranches very close to the threshold of instability.

(4) The long-range correlations between sidebranches, which suggest, following the model of Karma and Pelcé,[5] that the cell tips oscillate; however, we were not able to see this experimentally. Such a mechanism is plausible because the diffusion length l_d is much larger than the cell width λ (small Peclet number, $\mathrm{Pe}=\lambda/l_d \sim 0.1$). However, in order to explain the out-of-phase oscillation sidebranching, it might be necessary to assume that the cell-tip oscillation has a transverse component, in addition to the longitudinal component assumed by Karma and Pelcé in their calculations.

Let us now describe what happens when the layers make an angle α with the temperature gradient. We exclude from this discussion the unstable orientations close to $\alpha=0°$ and the faceted case ($\alpha > 10°$ and $\alpha \neq 90°$). At rest and at small velocities, the interface is smooth and stable [Fig. 2(a), $\alpha=45°$]. At a critical velocity V_c, a sinusoidal undulation occurs [Fig. 2(b)] whose amplitude slowly increases until the cells reach their stationary shape. The bifurcation is subcritical. At this velocity,

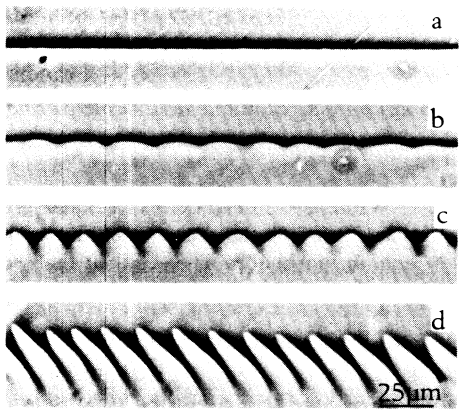

FIG. 2. The smectic layers oriented 45° with respect to the thermal gradient ($G=76$ K/cm); $\Delta T \approx 0.4$ K. (a) Flat, stationary interface; (b),(c) $V=0.8$ μm/s; (d) $V=0.95$ μm/s.

the cells are rounded [Fig. 2(c)] which means that the interface is locally stable (no forbidden orientations). At larger velocity, $V=1.2V_c$, the cells become asymmetric and develop facets and sharp tips that are, once more, a consequence of missing orientations in the equilibrium shape [Fig. 2(d)]. Careful observation of the cells shows that they move slowly along the unperturbed interface in the direction of the layers. We first measured the drift velocity V_d of the cells at onset [very-small-amplitude sinusoidal undulations; see Fig. 2(b)]. We observe that the ratio V_d/V (V is the pulling velocity) tends to zero as α tends to 0° or 90° and passes through a maximum close to 0.2 for $\alpha \approx 45°$ [Fig. 3(a)]. Note that this measurement is very difficult and becomes nearly impossible as α tends to 90° because the undulations immediately show faceting. We also measured the drift velocity V_d^* of the large-amplitude faceted cells at $V=1.2V_c$ [Fig. 3(b)]. In contrast to the previous case, V_d^*/V increases with α and surprisingly depends very little upon the size of the facet over the range of velocity we have explored. This behavior suggests that the physical processes at work may be different once the cells are faceted.

To explain the drift of the cells at onset, we propose two mechanisms.[6] The first concerns the anisotropy of kinetics of attachment of molecules on the interface (Coriell and Sekerka[7]). The second is specific to our system and is related to the anisotropy of the diffusion coefficients of an impurity in the smectic-A phase. As usual, we call $D_\parallel$ ($D_\perp$) the diffusion coefficient parallel (perpendicular) to the normal of the layers.

Coriell and Sekerka[7] analyzed the linear stability of a planar front, taking into account the kinetic anisotropy. The calculation was an extension of the well-known Mullins-Sekerka results.[8] They found

$$V_d/V=(\mu_x/\mu_T)(1/G\lambda), \quad (1)$$

where $\mu_x/\mu_T=(\partial\Delta T_{\mathrm{cin}}/\partial\alpha)_{V=\mathrm{const}}$ is a function of V and

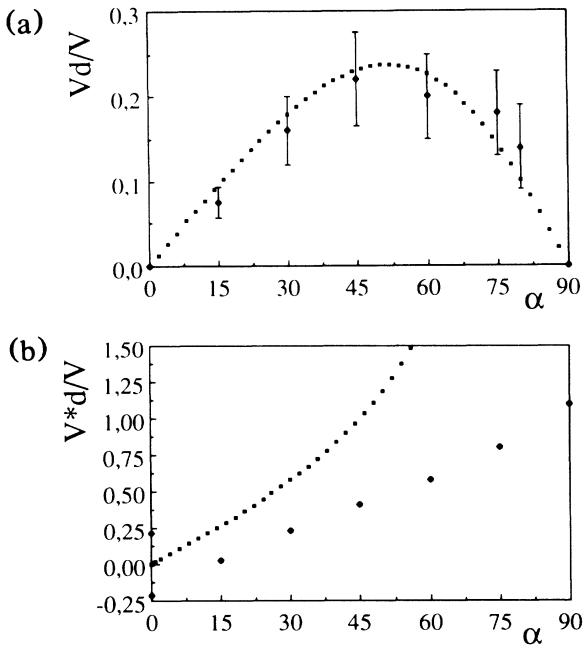

FIG. 3. (a) Drift velocity of the cells at onset vs the angle α. The dotted line is a fit by Eq. (2) with $D_\perp/D_\parallel \sim 1.6$. (b) Drift velocity of large-amplitude faceted cells ($V \sim 1.2 V_c$) vs α. The two points for $\alpha = 0°$ correspond to asymmetrical cells having their facet either on the left or on the right. The dotted line represents the geometrical limit corresponding to a very slow kinetics on the facet.

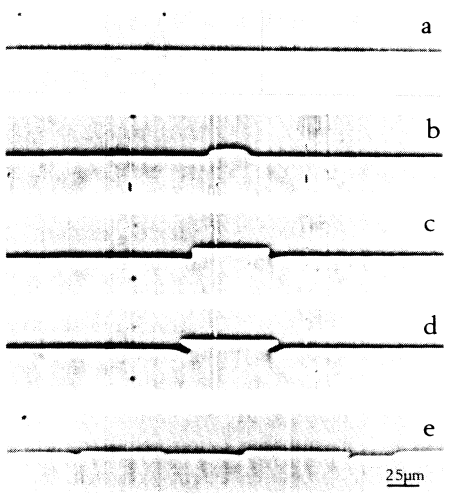

FIG. 4. Destabilization of a facet ($\alpha = 90°$, $\Delta T \approx 0.9$ K). (a) Facet at rest. (b)–(d)Nucleation and time evolution of two macrosteps of opposite signs; $G = 76$ K/cm and $V = 0.15$ μm/s: (b) $t = 0$, (c) $t = 6$ min, (d) $t = 7$ min. (e) Overall view of the front, $G = 63$ K/cm and $V = 0.25$ μm/s.

α that characterizes the anisotropy of kinetics. ΔT_{cin} is the kinetic undercooling at velocity V. G is the temperature gradient and λ is the undulation wavelength. They also showed that the surface-tension anisotropy does not give rise to a drift of the cells. We made an analogous calculation that took into account the diffusion anisotropy rather than the kinetic one. We found

$$V_d/V = (D_\perp - D_\parallel)\sin\alpha\cos\alpha/(D_\perp \cos^2\alpha + D_\parallel \sin^2\alpha) . \quad (2)$$

By convention, V_d is positive as the cells drift in the direction of the layers and negative otherwise. This relation shows that the drift velocity vanishes for $\alpha = 0°$ and 90° and passes through a maximum approximately equal to $(D_\perp - D_\parallel)/(D_\perp + D_\parallel)$ for $\alpha \approx 45°$ in the limit of small anisotropy. On the other hand, it follows from this model that V_d/V is independent of V, λ, and G, in contrast to the kinetic version.

In order to choose between these two models, we measured the ratio V_d/V as a function of λG by changing the temperature gradient and the impurity concentration. We found that it is nearly independent of λG (over the range 50–250 mK), and conclude that the propagation of the undulations is mainly due to the diffusion anisotropy in the smectic-A liquid crystal. On the other hand, the sign of V_d indicates that $D_\perp > D_\parallel$: Impurities diffuse more easily in the layers than perpendicular to them. The best fit to the experimental data of Fig. 3(a) with Eq. (2) leads to $D_\perp/D_\parallel \sim 1.6$. These data are compatible with the known values of diffusion coefficients in smectic-A phases.[9]

The case of large-amplitude faceted cells is much more difficult to analyze because it is no longer possible to make a perturbative calculation. The diffusion anisotropy and the kinetic effects are likely coupled. In the limit of very slow kinetics on the facet, the ratio V_d/V tends to its geometrical limit $\tan\alpha$. Experimentally, $V_d/V \ll \tan\alpha$ [Fig. 3(b)], which means that the facet grows and, possibly, that kinetic effects are negligible.

Let us now discuss the case $\alpha = 90°$, where the flat interface is itself a facet. At small velocities, the facet is stable [Fig. 4(a)]. At a critical velocity $V_c \sim 0.15$ μm/s, the facet destabilizes, but here the mechanism is quite different. We first observe the nucleation of macroscopic kinks (or macrosteps) which separate cold and hot facets [Fig. 4(b)]. These kinks appear randomly by pairs of opposite signs, without any periodicity. Just after nucleation, they are wide and of very small amplitude: They match tangentially the two facets. These kinks move and are unstable. They always travel from the hot facet to the cold one. Also, their shape changes with the amplitude. Wide at the beginning, they become steplike [Fig. 4(c)] and finally develop sharp edges [Fig. 4(d)]. They then propagate much faster than at the beginning, with a velocity close to the pulling velocity V, whereas before edge formation it was approximately $0.25V$. These mechanisms lead to the disappearance of the cold facet. The sequence begins again by nucleation and propagation of new macrosteps on the remaining facet.

An overall view of the front is shown in Fig. 4(e). Note that we never observed a stationary solution, whatever the velocity.

These observations agree qualitatively with the theoretical model of Bowley *et al.*[10] and Caroli, Caroli, and Roulet[11] on the fact that there exists a nonstationary solution consisting of alternating hot and cold facets. On the other hand, the theory does not explain the shape change of the macrosteps. To do that, it is perhaps necessary to consider the diffusion anisotropy in the smectic-A phase. Such calculations have yet to be done.

In conclusion, we have observed that the behavior of the Sm-A–Sm-B interface strongly depends upon its orientation with respect to the molecular layers. Our major result is that missing orientations of the equilibrium shape are still forbidden during growth, leading to an angular discontinuity at the cell tip. This boundary condition strongly affects the shape of the cells and could explain the nearly immediate development of sidebranches above the instability threshold. Let us recall that dendrites form at $V/V_c \approx 10$ in classical plastic crystals, while in our experiment, $V/V_c \approx 1.2$. The coherent sidebranches on many cells must also be emphasized and should be related to the unusually small value of the Peclet number. Finally, let us stress the crucial role played by diffusion anisotropy in explaining the drift of the cells.

We would like to thank C. Germain for providing us with the 4O.8 and J. Bechhoefer, C. Caroli, and J. S. Langer for fruitful discussions. This work was supported by Direction des Recherches, Etudes et Technique, Contract No. 88/1365.

[1]J. Bechhoefer, P. Oswald, A. Libchaber, and C. Germain, Phys. Rev. A **37**, 1691 (1988).

[2]P. Oswald, F. Melo, and C. Germain, "Smectic A-Smectic B Interface: Faceting and Surface Free Energy Measurement" (to be published).

[3]P. Oswald, J. Bechhoefer, and A. Libchaber, Phys. Rev. Lett. **58**, 2318 (1987); A. J. Simon, J. Bechhoefer, and A. Libchaber, Phys. Rev. Lett. **61**, 2574 (1988).

[4]M. Rabaud, S. Michalland, and Y. Couder, "Two Dynamical Regimes of a Linear Cellular Pattern: Spatio-Temporal Intermittency and Propagative Waves" (to be published).

[5]A. Karma and P. Pelcé, Phys. Rev. A **39**, 4162 (1989).

[6]Cell drift, presumably due to fluid flow, has been observed in germanium doped with gallium [R. Singh, A. F. Witt, and H. C. Gatos, J. Electrochem. Soc. **121**, 380 (1974)]. In our experiment, a flow is very difficult because of the layer structure of the smectic-A phase and we did not consider this possibility.

[7]S. R. Coriell and R. F. Sekerka, J. Cryst. Growth **34**, 157 (1976).

[8]W. W. Mullins and R. F. Sekerka, J. Appl. Phys. **35**, 444 (1965).

[9]G. J. Krüger, Phys. Rep. **82**, 229 (1982).

[10]R. Bowley, B. Caroli, C. Caroli, F. Graner, P. Nozières, and B. Roulet, J. Phys. (Paris) **50**, 1377 (1989).

[11]B. Caroli, C. Caroli, and B. Roulet, J. Phys. (Paris) **50**, 3075 (1989).

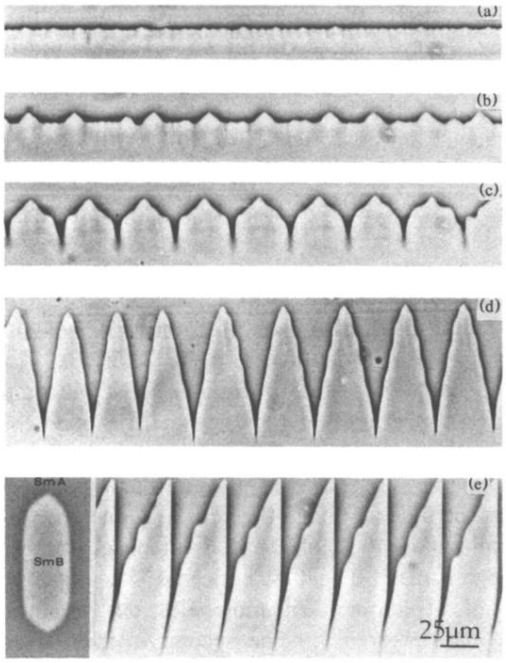

FIG. 1. Sm-A-Sm-B interface photographed via phase-contrast optics. The Sm-B is at the bottom and the Sm-A is at the top (the same in the other figures). For this sample, the temperature difference between liquidus and solidus lines is $\Delta T \approx 0.7$ K. The smectic layers are parallel to the temperature gradient, which is vertical ($G = 76$ K/cm). (a) Stationary interface: the hill-and-valley structure is clearly visible; (b), (c) $V = 0.38$ μm/s; (d),(e) $V = 0.45$ μm/s. Inset: A Sm-B monodomain in equilibrium with the Sm-A phase at constant temperature. The layers have the same orientation as those in (a)-(e).

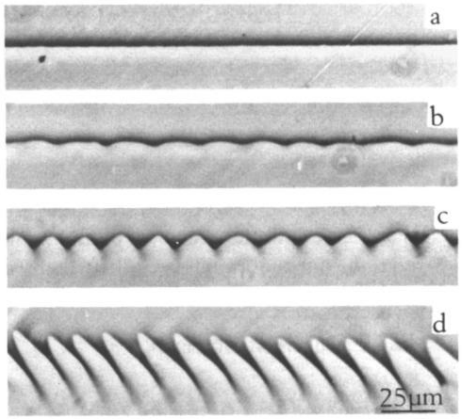

FIG. 2. The smectic layers oriented 45° with respect to the thermal gradient ($G=76$ K/cm); $\Delta T \approx 0.4$ K. (a) Flat, stationary interface; (b),(c) $V=0.8$ μm/s; (d) $V=0.95$ μm/s.

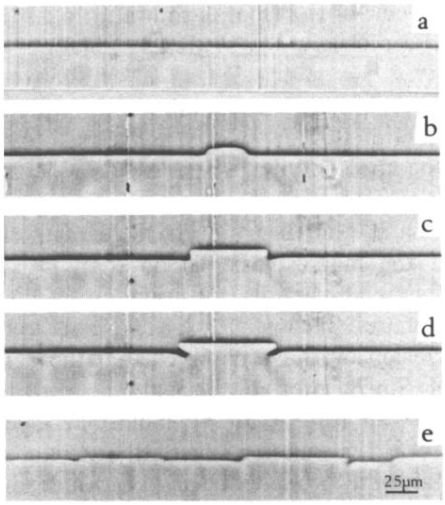

FIG. 4. Destabilization of a facet ($\alpha = 90°$, $\Delta T \approx 0.9$ K). (a) Facet at rest. (b)–(d)Nucleation and time evolution of two macrosteps of opposite signs; $G = 76$ K/cm and $V = 0.15$ μm/s: (b) $t = 0$, (c) $t = 6$ min, (d) $t = 7$ min. (e) Overall view of the front, $G = 63$ K/cm and $V = 0.25$ μm/s.